Effect of S and O on the growth of chemical-vapor deposition diamond (100) surfaces

Hiroyuki Tamura, Hui Zhou, Seiichi Takami, Momoji Kubo, and Akira Miyamoto[a)]
Department of Materials Chemistry, Graduate School of Engineering, Tohoku University, Aoba-yama 07, Sendai 980-8579, Japan

Mikka N.-Gamo and Toshihiro Ando
National Institute for Research in Inorganic Materials, 1-1 Namiki, Tsukuba, Ibaraki 305-0044, Japan

Sulfur and oxygen are known to improve the crystal quality of the chemical vapor deposition (CVD) diamond. In the CVD process, the sulfur is incorporated into the diamond crystal, while the oxygen is not incorporated. In the present study, first-principle calculations have been performed to investigate the effect of sulfur and oxygen on the growth mechanisms of CVD diamond (100) surfaces. The S and O atoms in the vapor are spontaneously inserted into the dimer bond on the diamond (100). The S and O insertions induce a compressive stress along the dimer bond and enhance the CH_2 bridging across the trough. In the case of oxygen, the on-top $C=O$ structure is spontaneously formed and it is considered to be desorbed from the surface during the CVD process. The S atom is considered to be incorporated into the diamond (100) lattice via the formation of 3-and 4-coordinated S on the surface. © *2001 American Institute of Physics.*

I. INTRODUCTION

Diamond is a potentially useful electronic device material due to its extreme properties, e.g., the highest hardness, high thermal conductivity, wide band gap, and high carrier mobility of p-type diamond. The p-type semiconducting diamond is obtained by boron doping, which is expected to realize high speed and high power devices due to its high carrier mobility.[1,2] However, an n-type semiconducting diamond is difficult to obtain regardless of the many attempts using donor dopants.[2–6] For example, nitrogen is incorporated into the diamond crystal; however, the donor level is so deep that the N-doped diamond is an insulator.[2] Phosphorus-doped diamond has also been produced, however, a high electron mobility and high crystal quality have never been achieved.[3–6] Therefore, the development of the n-type diamond is crucial to realize diamond devices.

Recently, Sakaguchi *et al.* have produced the n-type diamond by chemical-vapor deposition (CVD) growth of the (100) plane using a $CH_4/H_2/H_2S$ gas mixture.[7,8] The sulfur is considered to be incorporated into the diamond lattice as a donor dopant, where the concentration of S is very low.[7] The S-doped diamond exhibits a high electron mobility and high crystal quality and thus is expected to realize a practically useful n-type semiconductor. Hasegawa *et al.* have also produced the n-type diamond by sulfur-ion implantation.[9]

Oxygen is known to improve the crystal quality of the CVD diamond similar to sulfur, although oxygen is not incorporated into the diamond crystal during CVD.[10–14] The oxygen doping into the diamond crystal is possible only by the ion-implantation.[15] Diamond crystals have been successfully produced by the CVD using organic compounds [e.g., $CH_3OH, C_2H_5OH, CH_3COCH_3, C_2H_5OC_2H_5, (CH_3)_3N$],[10] and gas mixtures of $CH_4/H_2/O_2$,[11,12] $CH_4/H_2/H_2O$,[13] and $CO/O_2/H_2$.[14] The oxygen atom is believed to etch nondiamond carbon species during the CVD process.

From the previous first-principle calculations,[16] the donor level of the S-substituted diamond is shallower than those of the O-and N-substituted diamond, in agreement with the experiments. These calculations also revealed that O-substituted diamond is more stable than S-substituted diamond due to the smaller lattice distortion,[16] although oxygen cannot be incorporated into the diamond crystal during the CVD process.

In the typical diamond CVD, methane and a large amount of hydrogen are supplied in the source gas.[17–20] The CVD diamond (100) surfaces are known to be terminated by the 2×1 monohydride.[17–19] The structures and energetics of the hydrogenated diamond (100) surfaces have been exhaustively studied using various theoretical methods[21–36] due to their importance in the CVD growth. The reactions of diamond (100) surfaces with hydrocarbon species have also been investigated to elucidate the growth mechanisms.[37–48] Harris and Goodwin investigated the growth mechanisms of diamond (100) with CH_3 and H radicals using molecular mechanics calculations.[37] They reported that a CH_2 insertion into the 2×1 dimer bond on a terrace (dimer mechanism) and a CH_2 bridging across a trough at a step edge (trough mechanism) are considered to occur via several reaction steps. Kaukonen *et al.* investigated effects of nitrogen and boron on the CH_2 insertion into the dimer using the density-functional (DFT) calculations.[45]
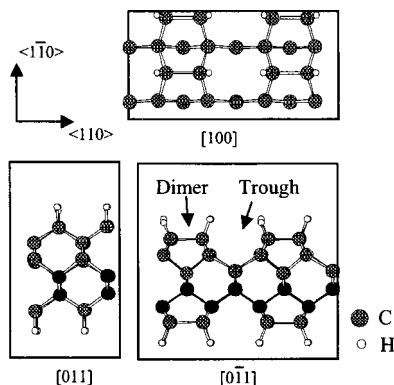
a)Electronic mail: miyamoto@aki.che.tohoku.ac.jp

FIG. 1. Slab model of the hydrogenated 2×1 diamond (100) surface represented by the 4×2 supercell, where the fixed carbon atoms are marked in black.

II. METHODS

The DFT calculations with a generalized gradient approximation (GGA), norm-conserving nonlocal pseudopotentials, and a plane-wave basis set were performed using the CASTEP code.[49] The plane-wave cutoff energy was set at 600 eV. The terrace of the hydrogenated 2×1 diamond (100) surface was represented by the slab model in the 4×2 supercell (Fig. 1). The details of the calculations are similar to those of the previous studies.[36,48]

The reliability of this method for the reaction of the diamond surface with oxygen has been proved in the previous study.[36] The accuracy for S-containing compounds was also proved by comparing the calculated equilibrium geometries and reaction energies (ΔE) with the experimental values. The calculated structural parameters of the S-containing compounds generally agree with the experimental values (Table I).[50] The binding energies of S tend to be systematically overestimated in the calculations (Table II), where the total energies of the S and O atom were calculated in the triplet state (total spin$=2$). This method is generally considered to be reliable for investigating the effect of sulfur and oxygen on the CVD reactions.

TABLE I. Structural parameters of molecules from calculations and experimental values (length [Å], angle [degree]).

		Calc.	Expt.
S$_2$	S–S	1.89	1.89
CS	C–S	1.52	1.53
CS$_2$	C–S	1.54	1.55
H$_2$S	H–S	1.35	1.34
	∠HSH	92	92
CH$_3$SH	C–S	1.80	1.82
	S–H	1.35	1.34
	C–H	1.09	1.09
	∠CSH	97	97
(CH$_3$)$_2$S	C–S	1.78	1.81
	∠CSC	99	99
C$_2$H$_4$S (ethylene sulfide)			
	C–C	1.47	1.48
	C–S	1.80	1.82
	∠CSC	48	48

III. RESULTS AND DISCUSSION

A. Effect of sulfur

Considering the plasma CVD of the diamond (100) using the CH$_4$/H$_2$/H$_2$S gas mixture, the reactions with the CH$_3$ radical, H radical, and atomic S were investigated. The calculated equilibrium geometries and reaction energies (ΔE) are summarized in Fig. 2 and Table III, respectively. The ΔE of the insertion of the atomic S into the dimer [Fig. 2(b)] is found to be exothermic with the value of -70 kcal/mol (the energy of atomic S was calculated in the triplet state). Therefore, this structure is considered to be stable in the CVD process. In this structure, the charge density of the highest occupied level is localized at the inserted S atom like a p orbital. The ΔE of the S insertion into C–C bonds from the second and third layers are found to be 37 and 125 kcal/mol, respectively. The S insertions into the lower layers are considered to be unfavorable due to the large lattice distortions. A similar tendency was found in the previous DFT calculations of the oxidations of the diamond (100).[36] The ΔE of the CH$_3$ adsorption on the inserted S atom [Fig. 2(i)] is found to be endothermic (27 kcal/mol). Therefore, the 3-coordinated S cannot be formed by the direct CH$_3$ adsorption on the S atom. The growth reactions are expected to preferentially proceed on the surrounded area.

The CVD growth of diamond is considered to proceed with the H abstraction from the diamond surface by the vapor H radical.[37,39,47,48] The previous DFT calculations revealed that the H abstractions from S$_B$ step edges at the $(2\times1)/(1\times2)$ domain boundaries of the diamond (100) surface are easier than those from the flat terraces,[48] where the ΔE of the H abstractions from the S$_B$ step edge and that from

Sulfur and oxygen are considered to affect the growth reactions during the CVD growth. A comparison between the effects of oxygen and those of sulfur on the growth mechanisms is also interesting, because their behaviors during the CVD process are expected to be different, though both of them are group VI elements. Their numbers of valence electrons are equal, while the electron–ion interactions and the core radii are different. The bond length of C–S is generally longer than that of C–O. In the present study, the effects of sulfur and oxygen on the growth reactions of the diamond (100) have been investigated using DFT calculations. There are several possible sulfur species (e.g., H$_2$S, HS, and atomic S) in the plasma CVD using the CH$_4$/H$_2$/H$_2$S gas mixture. In the present study, the atomic S is assumed to react with the diamond surface. As for the CVD using CH$_4$/H$_2$/O$_2$ gas mixture, the atomic O was considered as a reactive species.

TABLE II. Reaction energies (ΔE) of the vapor reaction of organic molecules from calculations and experimental values (kcal/mol).

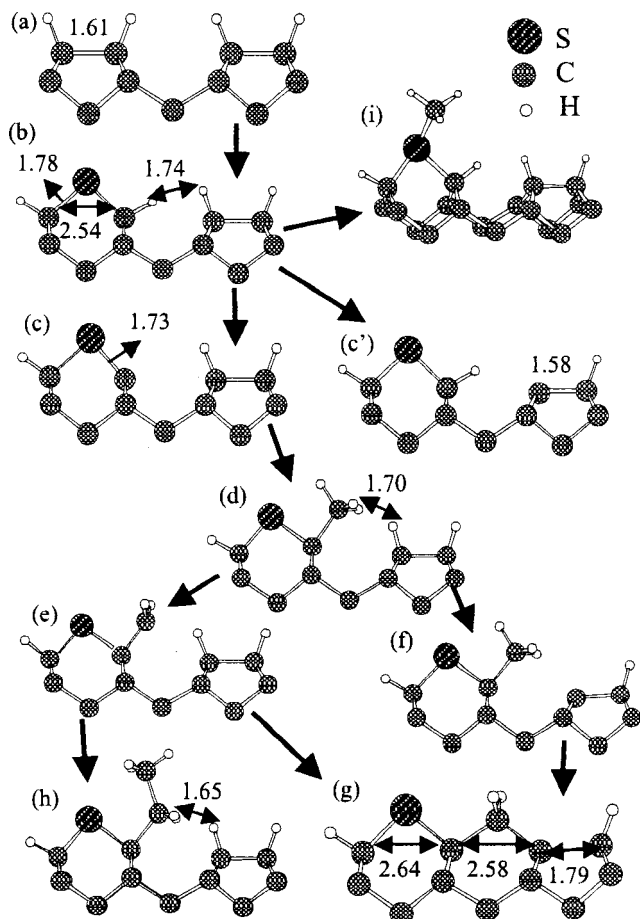|	Calc.	Expt.
H$_2$+S=H$_2$S	-79	-72
CH$_4$+S=CH$_3$SH	-59	-54
C$_2$H$_6$+S=(CH$_3$)$_2$S	-60	-56

FIG. 2. Reactions of the diamond (100) surface with H, CH$_3$, and S. Equilibrium geometries (in Å) of the (a) 2×1 monohydride dimer; (b) S-inserted dimer; dangling bond at the (c) S-inserted dimer and (c′) adjacent dimer; (d) CH$_3$ group at the S-inserted dimer; (e) CH$_2$ group at the S-inserted dimer; (f) dangling bond at the adjacent dimer; (g) CH$_2$ bridging across the trough; (h) C$_2$H$_5$ group at the S-inserted dimer; and (i) CH$_3$ adsorption on the S atom.
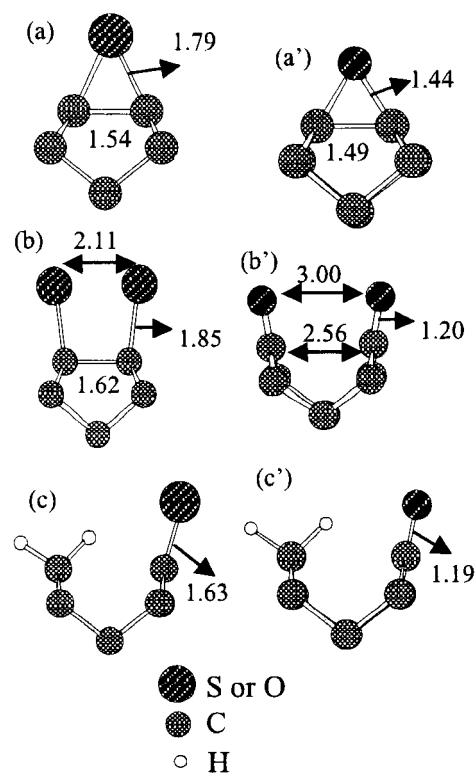

FIG. 3. Equilibrium geometries (in Å) of the (a) ethylene sulfide structure; (a′) epoxy structure; (b) on-top C–S; (b′) on-top C=O; (c) on-top C–S and (c′) C=O adjacent to dihydride.

the flat terrace were −9 and 1 kcal/mol, respectively. In the present study, the calculated ΔE of the H abstraction from the S-inserted dimer [Fig. 2(c)] is found to be −11 kcal/mol. Therefore, the S insertion into the dimer on the terrace

TABLE III. Reaction energies (ΔE) of the reaction of diamond (100) with CH$_3$ radical, H radical, and S atom as shown in Fig. 2. (1) S insertion into the dimer, H abstraction from the (2) S-inserted dimer and (3) adjacent dimer; (4) CH$_3$ adsorption at S-inserted dimer; (5) H abstraction from the CH$_3$ group at S-inserted dimer; (6) H abstraction from the adjacent dimer, CH$_2$ bridging with the (7) two-step H abstraction and (8) one-step H$_2$ desorption; (9) C$_2$H$_5$ formation at the S-inserted dimer, and (10) CH$_3$ adsorption on the S atom.

Reactions in Fig. 2	ΔE (kcal/mol)	
(a)+S=(b)	−70	(1)
(b)+H·=(c)+H$_2$	−11	(2)
(b)+H·=(c′)+H$_2$	−4	(3)
(c)+CH$_3$·=(d)	−35	(4)
(d)+H·=(e)+H$_2$	−23	(5)
(d)+H·=(f)+H$_2$	−16	(6)
(d)+2H·=(g)+2H$_2$	−116	(7)
(d)=(g)+H$_2$	−13	(8)
(e)+CH$_3$·=(n)	−55	(9)
(b)+CH$_3$·=(i)	27	(10)

enhances the H desorptions from the dimer up to that from the step edge. The distance between the H atoms from the dimers is decreased by the S insertion [Fig. 2(b)]; therefore, the steric repulsion is considered to enhance the H desorptions. The dangling bond at the S-inserted dimer [Fig. 2(c)] is more stable than that at the adjacent dimer [Fig. 2(c′)] due to the larger relaxation toward the plane structure.

After the second H desorption from the S-inserted dimer, the C–C length decreases and the equilibrium geometry, namely an ethylene–sulfide structure, is formed [Fig. 3(a)]. The ΔE of the second H abstraction (−45 kcal/mol) is more exothermic than that of the first one due to the pairing of the dangling bonds. The ΔE of the second H abstraction from the dimer is also known to be more exothermic than the first one due to the π bond formation.[17,26,48] Figure 3(b) shows the equilibrium geometry after the second S adsorption on the dimer (ΔE is −80 kcal/mol). The dimer bond is not dissociated by the second S adsorption in contrast to the oxidation of the dimer, in which on-top ketone (C=O) structures are formed and the dimer bond is dissociated [Fig. 3(b′)]. The on-top C–S structure as shown in Fig. 3(c) is less stable than the C–S–C structure [Fig. 2(b)] by 21 kcal/mol, where the stoichiometry is equal. The on-top C–S length is shorter than that of the single bonded one; however, it is too long to be stabilized by the π bond. In the case of oxygen, the on-top C=O structure [Fig. 3(c′)] is less stable than the C–O–C structure [Fig. 3(b′)] by 5 kcal/mol. The C–O length is shorter than the C–S length, thus, the π bond formation is more favorable.
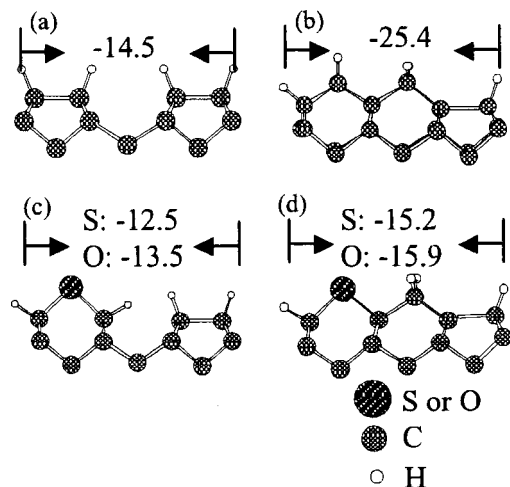
FIG. 4. Stress tensor (in GPa) along the dimer bond of (a) 2×1 monohydride dimer; (b) CH_2 bridging at the step edge; (c) S- (O-) inserted dimer; and (d) CH_2 bridging at the S- (O-) inserted dimer, where the negative and positive values denote the tensile and compressive stresses, respectively.

In the growth process at the step edge, the CH_3 radical is adsorbed on the dangling bond at the step edge, then the CH_2 group bridges across the trough with H desorptions.[37,48] Similar growth reactions are considered to proceed at the S-inserted dimer. The ΔE of the CH_3 adsorption on the dangling bonds at the S-inserted dimer is found to be -35 kcal/mol, which is less exothermic than that at the dimer on the flat terrace (-84 kcal/mol[48]) due to the steric repulsion between the CH_3 group and adjacent H atom [Fig. 2(d)]. A similar tendency is found in the previous calculation of the CH_3 adsorption at the step edge.[48] The CH_2 bridging across the trough is considered to occur with two-step H abstractions or one-step H_2 desorption.[48] At the S-inserted dimer, the H desorptions from the CH_3 group [Fig. 2(e)] and adjacent dimer [Fig. 2(f)] are enhanced by the steric repulsion. The CH_2 group spontaneously bridges across the trough [Fig. 2(g)] with the H desorptions. The ΔE of all the reactions from the S insertion to the CH_2 bridging [Figs. 2(a)–2(g)] are found to be exothermic; therefore, these reactions can proceed during the CVD growth. These reactions are similar to the CH_2 bridging across the trough at the step edge (trough mechanism).[37,48] In the case of the reactions on the terrace without the S insertion, the CH_2 insertion into the dimer bond (dimer mechanism) is considered to proceed.[37,48] The S insertion into the dimer bond on the terrace is considered to induce the CH_2 bridging across the trough rather than the CH_2 insertion into the dimer bond.

The C_2H_5 group is considered to be formed as a by-product by the CH_3 adsorption on the CH_2 group.[48] The C_2H_5 formation during the dimer mechanism inhibits the CH_2 insertion into the dimer bond, and that during the trough mechanism inhibits the CH_2 bridging across the trough. The previous DFT calculations revealed that the C_2H_5 formation during the trough mechanism at the step edge is less favorable than that during the dimer mechanism on the terrace due to the steric repulsion.[48] The ΔE of the C_2H_5 formation at the S-inserted dimer [Fig. 2(h)] is found to be -55 kcal/mol, which are less exothermic than that on the flat terrace (-77
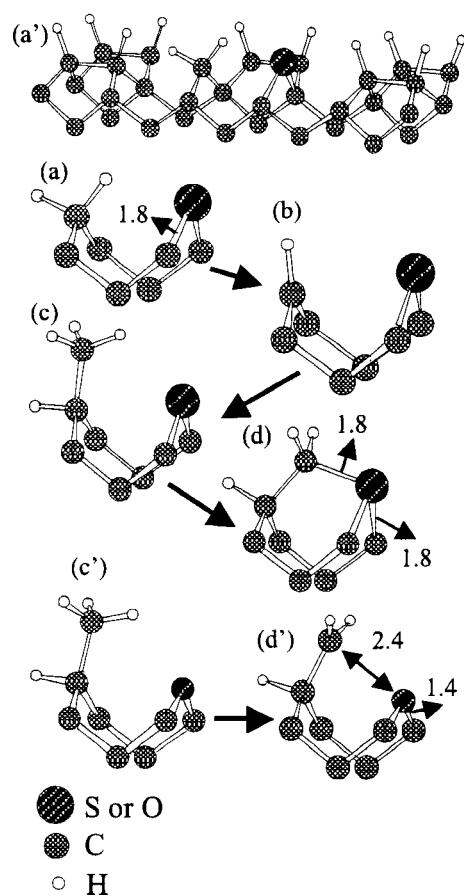

FIG. 5. Reaction path of the formation of 3-coordinated S and O on the diamond (100) surface. Equilibrium geometries (in Å) of the (a)(a′) dihydride adjacent to C–S–C; (b) dangling bond adjacent to C–S–C, adsorbed CH_3 group (c) adjacent to C–S–C, and (c′) adjacent to C–O–C, CH_2 group, (d) adjacent to C–S–C, and (d′) adjacent to C–O–C, where the structure of the surrounded area is shown in (a′).

kcal/mol). Therefore, the C_2H_5 group at the S-inserted dimer is less stable than that on the flat terrace due to the steric repulsion similar to that at the step edge.

The effects of the S insertion on the stress tensor were investigated (Fig. 4). In the case of the dimer arrays on the flat terrace [Fig. 4(a)], the calculated stress tensors parallel and perpendicular to the dimer bond are -14.5 and -0.8 GPa, respectively. This means that there is a significant tensile stress along the dimer bond. Figure 4(b) shows the equilibrium geometry of the step edge bridged by the CH_2.[48] The CH_2 bridging at the step edge significantly increases the tensile stress along the dimer bond. The S insertion is found to decrease the tensile stress along the dimer bond [Fig. 4(c)]; in other words, the S insertion induces a compressive stress. The tensile stress of the CH_2-bridged structure at the S-inserted dimer [Fig. 4(d)] is found to be lower than that at the step edge due to the compressive stress by the S insertion. These results indicate that the compressive stress by the S insertion stabilizes the CH_2-bridged structure.

B. Sulfur incorporation

Further reactions to incorporate sulfur into the diamond lattice were investigated (Fig. 5, 6, and Table IV, V). The
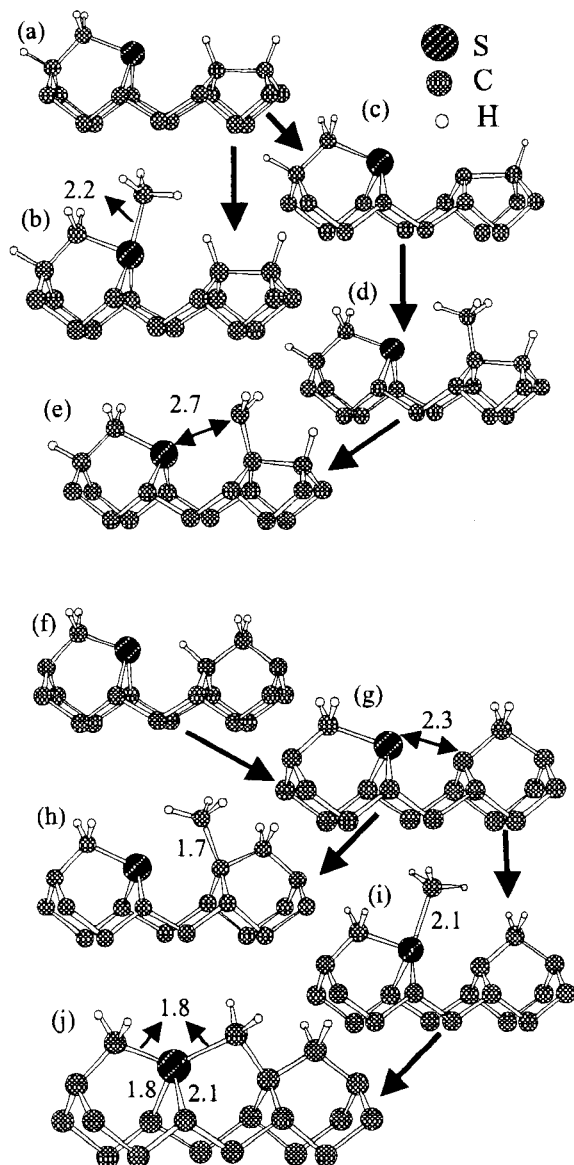
FIG. 6. Reaction path of the formation of 4-coordinated S on the diamond (100) surface. Equilibrium geometries (in Å) of the (a) 3-coordinated S; (b) CH$_3$ adsorbed on S; (c) dangling bond at the dimer; (d) CH$_3$ group at the dimer; (e) CH$_2$ group at the dimer; (f) CH$_2$-inserted dimer adjacent to the 3-coordinated S; (g) H abstraction from the CH$_2$-inserted dimer; (h) CH$_3$ group at the CH$_2$-inserted dimer; (i) CH$_3$ group on S; and (j) 4-coordinated S.

TABLE IV. Reaction energies (ΔE) of the formation of 3-coordinated S and O on the diamond (100) surface as shown in Fig. 5. (1) H abstraction from the dihydride; (2) CH$_3$ adsorption adjacent to the C–S–C; (3) H abstraction from the CH$_3$ group adjacent to C–S–C; (4) H abstraction from the CH$_3$ group adjacent to C–O–C.

Reactions in Fig. 5	ΔE (kcal/mol)	
(a)+H·=(b)+H$_2$	−26	(1)
(b)+CH$_3$·=(c)	−43	(2)
(c)+H·=(d)+H$_2$	−17	(3)
(c′)+H·=(d′)+H$_2$	−8	(4)

2-coordinated S [Fig. 2(i)] is endothermic. Since the surface dangling bond is localized at the 3-coordinated S atom (total spin=1), it is more reactive than the 2-coordinated S at which the lone pair is localized (total spin=0). The CH$_2$ bridging between the 3-coordinated S and adjacent dimer was investigated [Figs. 6(a)–6(e)]. However, at this stage, the CH$_2$ bridging is found to be unfavorable due to the long C–S distance [Fig. 6(e)]. Therefore, this 3-coordinated S remains on the surface while the surrounded area is grown by the CH$_2$ insertions into the dimer and the CH$_2$ bridging across the trough.

Then, we investigated the reactions after the growth of surrounded area. After the CH$_2$ insertions at both sides of 3-coordinated S, the CH$_2$ row is formed, except a trough remains at the S [Fig. 6(f)]. The 4-coordinated S is expected to be formed by the CH$_2$ bridging across this trough. The H abstraction from the edge of the CH$_2$-inserted dimer [Fig. 6(g)] is found to be much more exothermic (−48 kcal/mol) than those from the terrace due to the steric repulsion with the S atom. The CH$_3$ adsorption on this C atom [Fig. 6(h)] is found to be endothermic due to the steric repulsion between the CH$_3$ and S, whereas the CH$_3$ adsorption on the S atom [Fig. 6(i)] is found to be exothermic, because the steric repulsion is small due to the large equilibrium S–CH$_3$ bond length. Then, the CH$_2$ bridging spontaneously occurs via the H abstraction from this CH$_3$ group. According to the above reactions, the S atom is spontaneously incorporated into the second layer of the diamond (100) surface [Fig. 6(i)]. In this structure, the one C–S bond length is longer than the others. The similar tendency was also found in the previous DFT calculations of the S-substituted bulk diamond.[16] The hydro-

direct CH$_3$ adsorption on the S atom [Fig. 2(i)] is unfavorable and thus the C–S–C structure is expected to remain on the surface while the growth reactions proceed on the surrounded area. The surface is expected to be covered with the 2×1 monohydride dimer unless an odd dihydride remains adjacent to C–S–C [Fig. 5(a′)]. The CH$_2$ bridging is considered to proceed at the S atom via the H abstraction from the dihydride [Fig. 5(b)], CH$_3$ adsorption on this dangling bond [Fig. 5(c)], and H abstraction from this CH$_3$ group [Fig. 5(d)]. In this case, the CH$_2$ group is restrained by the surrounded diamond lattice and thus the 3-coordinated S is spontaneously formed.

The CH$_3$ adsorption on the 3-coordinated S atom [Fig. 6(b)] is found to be exothermic, although that on the

TABLE V. Reaction energies (ΔE) of the formation of 4-coordinated S on the diamond (100) surface as shown in Fig. 6. (1) CH$_3$ adsorption on the 3-coordinated S; (2) H abstraction from the dimer; (3) CH$_3$ adsorption on the dimer; (4) H abstraction from the CH$_3$ group; (5) H abstraction from the CH$_2$-inserted dimer; (6) CH$_3$ adsorption on the CH$_2$-inserted dimer; (7) CH$_3$ adsorption on the S atom; (8) CH$_2$ bridging between the S and C atom.

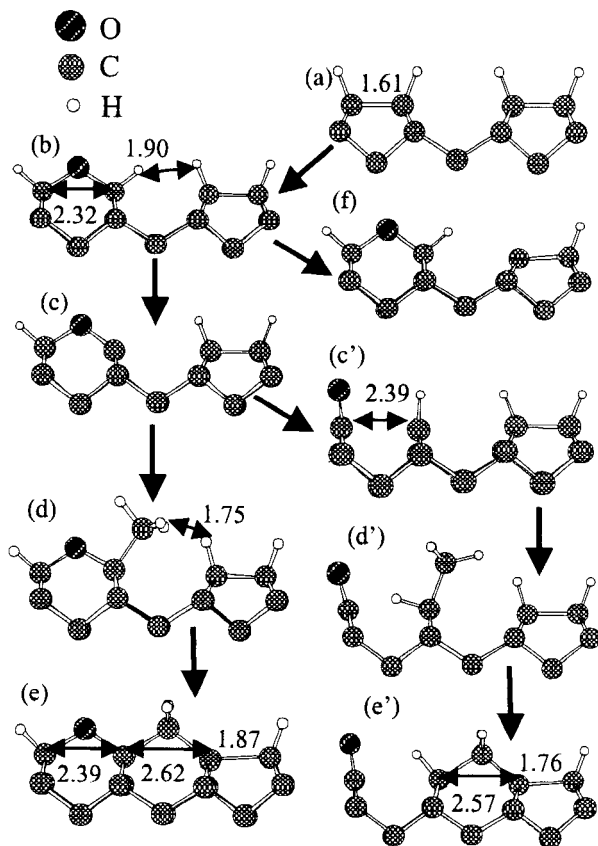| Reactions in Fig. 6	ΔE (kcal/mol)	
(a)+CH$_3$·=(b)	−29	(1)
(a)+H·=(c)+H$_2$	−13	(2)
(c)+CH$_3$·=(d)	−59	(3)
(d)+H·=(e)+H$_2$	−14	(4)
(f)+H·=(g)+H$_2$	−48	(5)
(g)+CH$_3$·=(h)	27	(6)
(g)+CH$_3$·=(i)	−9	(7)
(i)+H·=(j)+H$_2$	−23	(8)

FIG. 7. Reactions of the diamond (100) surface with H, CH$_3$, and O. Equilibrium geometries (in Å) of the (a) 2×1 monohydride dimer; (b) O-inserted dimer; (c) dangling bond at the O-inserted dimer; (c′) dangling bond adjacent to the C=O group; (d) CH$_3$ group at the O-inserted dimer; (d′) CH$_3$ group adjacent to the C=O group; CH$_2$ bridging (e) adjacent to the O-inserted dimer, and (e′) adjacent to the C=O group; and (f) dangling bond at the adjacent dimer.

genated top layer is expected to react with the CH$_3$ and H radicals similar to the conventional CVD growth. Therefore, the S atom is expected to be spontaneously incorporated into the bulk diamond lattice; in other words, the S-substituted diamond is obtained via the above reactions.

C. Effect of oxygen

During the CVD process using CH$_4$/H$_2$/O$_2$ gas mixture, the diamond (100) surface is considered to react with the CH$_3$ radical, H radical, and atomic O in the vapor phase. Based on the previous experimental[51,52] and theoretical[34–36,53–56] studies, the cyclic ether structure (C–O–C) is formed on the diamond (100) by the O insertion into the dimer bond. The oxidations of lower layers of the diamond surfaces are unfavorable due to the large lattice distortions.[36] Figure 7(b) and Table VI show the calculated equilibrium geometry of the O-inserted dimer, where the ΔE of the insertion of the atomic O is found to be −115 kcal/mol. Because the equilibrium length of the C–O bond is shorter than that of the C–S bond, the calculated C–C distance of the O-inserted dimer (2.32 Å) is shorter than that of the S-inserted dimer (2.54 Å). The O insertion is found to weaken the tensile stress along the dimer bond (before: −14.5, after: −13.5 GPa), similar to the S insertion (Fig. 4).

TABLE VI. Reaction energies (ΔE) of the reaction of diamond (100) with CH$_3$ radical, H radical, and O atom as shown in Fig. 7. (1) O insertion into the dimer bond; (2) H abstraction from the O-inserted dimer; (3) H abstraction from the adjacent dimer; (4) CH$_3$ adsorption at the O-inserted dimer; CH$_2$ bridging adjacent to the C–O–C with the (5) 2-step H abstraction; and (6) one-step H$_2$ desorption; (7) C=O group formation; (8) CH$_3$ adsorption adjacent to C=O, CH$_2$ bridging adjacent to the C=O with the (9) two-step H abstraction and (10) one-step H$_2$ desorption.

Reaction in Fig. 7	ΔE (kcal/mol)	
(a)+O=(b)	−115	(1)
(b)+H·=(c)+H$_2$	−7	(2)
(b)+H·=(f)+H$_2$	−1	(3)
(c)+CH$_3$·=(d)	−58	(4)
(d)+2H·=(e)+2H$_2$	−84	(5)
(d)=(e)+H$_2$	19	(6)
(c)=(c′)	−4	(7)
(c′)+CH$_3$·=(d′)	−48	(8)
(d′)+2H·=(e′)+2H$_2$	−94	(9)
(d′)=(e′)+H$_2$	9	(10)

The adsorption of the CH$_3$ radical on the inserted O atom is found to be unstable; in this case, the equilibrium geometry could not be found. The 3-coordinated S and O on the diamond (100) surfaces cannot be formed by the direct CH$_3$ adsorption.

The ΔE of the H abstraction from the O-inserted dimer (−7 kcal/mol) and adjacent dimer (−1 kcal/mol) are more exothermic than that from the dimer on the flat terrace (1 kcal/mol).[48] The distance between the H atom from the O-inserted dimer and that from the adjacent dimer decreases to 1.90 Å [Fig. 7(b)], which is larger than that in the case of the S insertion (1.74 Å). Therefore, the effect of steric repulsion due to the O insertion is smaller than that due to the S insertion. After the second H abstraction from the O-inserted dimer, the dimer bond length decreases and the equilibrium geometry, namely an epoxy structure, is formed [Fig. 3(a′)]. The ΔH of the second H abstraction (−20 kcal/mol in Table II) is more exothermic than that of the first one (−7 kcal/mol) due to pairing of the dangling bonds similar to the case of sulfur.

The CH$_3$ adsorption [Fig. 7(d)] and the CH$_2$ bridging [Fig. 7(e)] proceed at the C–O–C similar to the case of C–S–C. Since the O insertion induces a compressive stress along the dimer bond, the tensile stress after the CH$_2$ bridging (−15.9 GPa) is lower than that after the CH$_2$ bridging at the step edge (−25.4 GPa) similar to the case of the S insertion. The ΔE of the C$_2$H$_5$ group formation at the O-inserted dimer is found to be −73 kcal/mol, which is less stable than that at the flat terrace (−77 kcal/mol[48]) and more stable than that at the S-inserted dimer (−55 kcal/mol).

Both the S and O insertions into the dimer bond are considered to induce the CH$_2$ bridging across the trough. These reaction mechanisms are similar to that at the S$_B$ step.[37,48] In these cases, the H desorptions are more favorable and the adsorbed species (e.g., CH$_3$ and C$_2$H$_5$) is less stable due to the steric repulsions.

The on-top C=O structure is known to be stable on the diamond (100) surface.[36,51,52] Therefore, the CH$_2$ bridging with the C=O group formation was also investigated. The

C=O structure [Fig. 7(c')] is formed via the H abstraction from O-inserted dimer and C–O bond dissociation. The ΔE of the C=O formation by the C–O dissociation is exothermic, with the value of -4 kcal/mol. The CH_3 radical is adsorbed at the dangling bond adjacent to the C=O group [Fig. 7(d')]. Then, the CH_2 group is bridged across the trough via the H desorptions [Fig. 7(e')]. The CH_2-bridged structure adjacent to the C=O group [Fig. 7(e')] is more stable than that adjacent to the C–O–C group [Fig. 7(e)] by 5 kcal/mol, where the stoichiometry is equal. The difference in energies between the C=O and C–O–C structures is not very large; therefore, they are considered to coexist during the CVD process.

Pehrsson observed the thermal desorptions of the oxygen-containing species from the diamond (100) surface and revealed that the C=O group preferentially desorbs while the C–O–C groups remain on the surface.[51] In the present calculations, the ΔE of the C=O desorption from the diamond surface is found to be endothermic (63 kcal/mol). The ΔE of the CO_2 desorption with the vapor O atom is found to be more exothermic (-90 kcal/mol). Therefore, the atomic O in the vapor phase is considered to enhance the CO_2 desorptions during the CVD process. The CVD growth proceeds at high temperatures and thus the inserted oxygen is expected to be desorbed from the surface via the C=O group formation.

The formation of 3-coordinated O was investigated similar to sulfur [Figs. 5(c') and 5(d')]. In this case, the repulsion between the CH_2 group and the 2-coordinated O atom is so strong that the 3-coordinated O is not formed and the CH_2 group keeps the planer structure [Fig. 5(d')]. An antibonding orbital (p–p σ^*) between the CH_2 and O atom is found in the highest occupied level of this structure. The O incorporation into the CVD diamond is considered to be less favorable than the S incorporation due to the unstable intermediate structure during the growth reactions, although the O-substituted bulk diamond is more stable than the S-substituted one due to the smaller lattice distortion.[16]

IV. CONCLUSIONS

The DFT calculations revealed the effects of sulfur and oxygen on the growth mechanisms of the CVD diamond (100) surfaces as follows.

(1) The S and O atoms are spontaneously inserted into the dimer bond on the diamond (100) surface.
(2) The S (O) insertions enhance the H desorption from the dimer.
(3) The CH_3 and C_2H_5 groups at the S-(O-) inserted dimer are less stable than those on the flat terrace due to the steric repulsion.
(4) The S-(O) insertions induce a compressive stress along the dimer bond and decrease the tensile stress of the CH_2-bridged structure.

The growth reactions at the S- (O-) inserted dimer are generally similar to those at the S_B step edge. The S- (O) insertions are expected to induce the trough mechanism (i.e., CH_2 bridging across the trough) rather than the dimer mecha-

nism (i.e., CH_2 insertion into the dimer bond). This tendency makes the by-products (e.g., C_2H_5 group) unstable.

The significant difference between sulfur and oxygen is the stabilities of the on-top and 3-coordinated structures on the diamond surface. In the case of oxygen, the on-top C=O structure is spontaneously formed and it is considered to be desorbed from the surface during the CVD process. Moreover, the 3-coordinated O, which is an intermediate of the O incorporation, is relatively unstable compared with sulfur. Therefore, the oxygen incorporation into the CVD diamond is considered to be unfavorable as observed in the experiments. In the case of sulfur, the on-top structure is relatively unstable. The S atom is considered to be incorporated into the diamond lattice via the formation of 3- and 4-coordinated S on the surface. From the previous calculations for bulk diamond,[16] the O substitution is more favorable than the S substitution due to the smaller lattice distortion. In the case of the CVD growth, however, the S incorporation is more favorable than the O incorporation due to the stability of the intermediates on the surface.

[1] S. Yamanaka *et al.*, Jpn. J. Appl. Phys. **37**, L1129 (1998).
[2] A. T. Collins, in *Properties and Growth of Diamond*, edited by G. Davies (INSPEC, the Institution of Electronical Engineers, London, UK, 1993), and A. T. Collins, Mater. Res. Soc. Symp. Proc. **162**, 3 (1990).
[3] N. Fujimori, T. Imai, H. Nakahata, H. Shiomi, and Y. Nishibayashi, Mater. Res. Soc. Symp. Proc. **162**, 23 (1990).
[4] A. E. Alexenko and B. V. Spitsyn, Diamond Relat. Mater. **1**, 705 (1992).
[5] S. Koizumi, M. Kamo, Y. Sato, H. Ozaki, and T. Inuzuka, Appl. Phys. Lett. **71**, 1065 (1997).
[6] T. Saito *et al.*, Jpn. J. Appl. Phys. **37**, L543 (1998).
[7] I. Sakaguchi, M. N.-Gamo, Y. Kikuchi, E. Yasu, H. Haneda, T. Suzuki, and T. Ando, Phys. Rev. B **60**, 2139 (1999).
[8] M. N-Gamo, C. Xiao, Y. Zhang, E. Yasu, Y. Kikuchi, I. Sakaguchi, T. Suzuki, Y. Sato, and T. Ando, Thin Solid Films (in press).
[9] M. Hasegawa, D. Takeuchi, S. Yamanaka, M. Ogura, H. Watanabe, N. Kobayashi, H. Okushi, and K. Kajimura, Jpn. J. Appl. Phys. **38**, L1519 (1999).
[10] Y. Hirose and Y. Terasawa, Jpn. J. Appl. Phys. **25**, L519 (1986).
[11] T. Kawato, K. Kondo, Jpn. J. Appl. Phys. **26**, 1429 (1987).
[12] Y. Liou, R. Weimer, D. Knight, and R. Messier, Appl. Phys. Lett. **56**, 437 (1990).
[13] Y. Saito, K. Sato, H. Tanaka, K. Fujita, and S. Matuda, J. Mater. Sci. **23**, 842 (1988).
[14] Y. Muranaka, H. Yamashita, and H. Miyadera, J. Appl. Phys. **69**, 8145 (1991).
[15] J. F. Prins, Phys. Rev. B **61**, 7191 (2000).
[16] H. Zhou, Y. Yokoi, H. Tamura, S. Takami, M. Kubo, A. Miyamoto, M. N-Gamo, and T. Ando, Jpn. J. Appl. Phys. **40**, 2830 (2001).
[17] M. P. D'Evelyn, in *Handbook of Industrial Diamonds and Diamond Films*, edited by M. A. Prelas, G. Popovici, and L. K. Bigelow (Dekker, New York, 1998), pp. 89–146.
[18] F. G. Celii and J. E. Butler, Annu. Rev. Phys. Chem. **42**, 643 (1991).
[19] B. B. Pate, Surf. Sci. **165**, 83 (1986).
[20] T. Tsuno, T. Tomikawa, S. Shikata, T. Imai, and N. Fujimori, Appl. Phys. Lett. **64**, 572 (1994).
[21] D. W. Brenner, Phys. Rev. B **42**, 9458 (1990).
[22] Y. L. Yang and M. P. D'Evelyn, J. Am. Chem. Soc. **114**, 2796 (1992); J. Vac. Sci. Technol. A **10**, 978 (1992).
[23] W. S. Verwoerd, Surf. Sci. **103**, 404 (1981); **108**, 153 (1981).
[24] S. P. Mehandru and A. B. Anderson, Surf. Sci. **248**, 369 (1991).
[25] X. M. Zheng and P. V. Smith, Surf. Sci. **256**, 1 (1991).
[26] T. I. Hukka, T. A. Pakkanen, and M. P. D'Evelyn, J. Phys. Chem. **98**, 12420 (1994).
[27] S. Skokov, C. S. Carmer, B. Weiner, and M. Frenklach, Phys. Rev. B **49**, 5662 (1994).
[28] S. H. Yang, D. A. Drabold, and J. B. Adams, Phys. Rev. B **48**, 5261 (1993).
[29] Th. Frauenheim, U. Stephan, P. Blaudeck, D. Porezag, H.-G. Busmann, W.

Zimmermann-Edling, and S. Lauer, Phys. Rev. B **48**, 18189 (1993).

[30] C. Kress, M. Fiedler, W. G. Schmidt, and F. Bechstedt, Phys. Rev. B **50**, 17697 (1994).

[31] J. Furthmüller, J. Hafner, and G. Kresse, Phys. Rev. B **50**, 15606 (1994); **53**, 7334 (1996).

[32] B. N. Davidson and W. E. Pickett, Phys. Rev. B **49**, 11253 (1994).

[33] M. D. Winn, M. Rassinger, and J. Hafner, Phys. Rev. B **55**, 5364 (1997).

[34] J. L. Whitten and P. Cremaschi, Appl. Surf. Sci. **75**, 45 (1994).

[35] M. J. Rutter and J. Robertson, Phys. Rev. B **57**, 9241 (1998).

[36] H. Tamura, H. Zhou, K. Sugisako *et al.*, Phys. Rev. B **61**, 11025 (2000).

[37] S. J. Harris and D. G. Goodwin, J. Phys. Chem. **97**, 23 (1993).

[38] D. R. Alfonso, S. E. Ulloa, and D. W. Brenner, Phys. Rev. B **49**, 4948 (1994).

[39] S. Skokov, B. Weiner, and M. Frenklach, J. Phys. Chem. **98**, 7073 (1994); **99**, 5616 (1994).

[40] M. Frenklach, S. Skokov, and B. Weiner, Nature (London) **372**, 535 (1994).

[41] T. I. Hukka, T. A. Pakkanen, and M. P. D'Evelyn, Surf. Sci. **359**, 213 (1996).

[42] K. Larsson, S. Lunell, and J. O. Carlsson, Phys. Rev. B **48**, 2666 (1993).

[43] M. H. Tsai and Y. Y. Yeh, Phys. Rev. B **58**, 2157 (1998).

[44] D. R. Alfonso, S. H. Yang, and D. A. Drabold, Phys. Rev. B **50**, 15369 (1994).

[45] M. Kaukonen, P. K. Sitch, G. Jungnickel, R. M. Nieminen, S. Poykko, D.

Porezag, and Th. Frauenheim, Phys. Rev. B **57**, 9965 (1998).

[46] E. J. Dawnkaski, D. Srivastava, and B. J. Garrison, J. Chem. Phys. **102**, 9401 (1995); **104**, 5997 (1996).

[47] C. C. Battaile, D. J. Srolovitz, I. I. Oleinik, D. G. Pettifor, A. P. Sutton, S. J. Harris, and J. E. Butler, J. Chem. Phys. **111**, 4291 (1999).

[48] H. Tamura, H. Zhou, Y. Hirano, S. Takami, M. Kubo, R. V. Belosludov, A. Miyamoto, A. Imamura, M. N. Gamo, and T. Ando, Phys. Rev. B **62**, 16995 (2000).

[49] M. C. Payne, M. P. Teter, D. C. Allan, T. A. Arias, and J. D. Joannopoulos, Rev. Mod. Phys. **64**, 1045 (1992).

[50] L. E. Sutton, *Tables of Interatomic Distance and Configuration in Molecules and Ions* (The Chemical Society Spatial Publication, No. 11, 18, London, 1958, 1965); J. B. Pedley, and J. Rylance, *Computer Analyzed Thermochemical Data: Organic and Organometallic Compounds* (University of Sussex, Sussex, 1977).

[51] P. E. Pehrsson, Electrochem. Soc. Proc. **95−194**, 436 (1995).

[52] M. Z. Hossain, T. Kubo, T. Aruga, N. Takagi, T. Tsuno, N. Fujimori, and N. Nishijima, Surf. Sci. **436**, 63 (1999).

[53] P. Badziag and W. S. Verwoerd, Surf. Sci. **183**, 469 (1987).

[54] X. M. Zheng and P. V. Smith, Surf. Sci. **262**, 219 (1992).

[55] S. Skokov, B. Weiner, and M. Frenklach, Phys. Rev. B **49**, 11374 (1994); **55**, 1895 (1997).

[56] Y. Okamoto, Phys. Rev. B **58**, 6760 (1998).